

An Integrated Used Fuel Disposition and Generic Repository Model for Fuel Cycle Analysis

PhD Oral Examination

Kathryn D. Huff
PhD Candidate

University of Wisconsin-Madison

August 16, 2013





Outline

① Motivation

- Future Fuel Cycle Options
- Geologic Disposal Concept Options
- Fuel Cycle Simulator Capabilities

② Modeling Paradigm

- Cyder Overview
- Thermal Transport in Cyder
- Radionuclide Transport in Cyder

③ Demonstration

- Radionuclide Transport Toy Cases
- Radionuclide Transport Validation Cases
- Thermal Transport Toy Cases
- Thermal Transport Validation Cases

④ Conclusion



Top Level Fuel Cycle Simulators

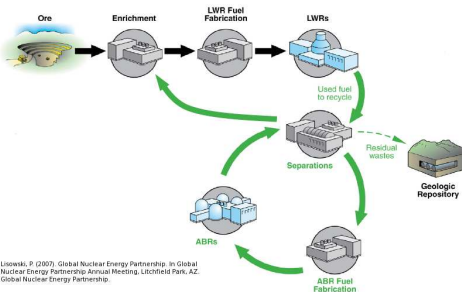


Figure 1 : Top level simulators are intended to model the collective behavior of various fuel cycle decisions and strategies [24].



Future Fuel Cycle Options

Domestic Fuel Cycle Options

Title	Description	Challenges
Open	Once Through Current US PWR Fleet No Separations No Recycling Higher Burnups	High Temperatures, Volumes
Modified Open	Partial Recycling Next Gen. PWR Fleet Limited Separations Limited Transmutation Advanced Fuel Forms HLW treatment	Both high volumes and variable spent fuel streams
Closed	Full Recycling Full Separations Full Recycling VHTGR, SFRs, other transmutation HLW treatment	Variable spent fuel streams

Table 1 : Domestic Fuel Cycle Options



Disposal Geology Options Considered

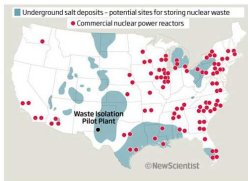


Figure 2 : U.S. Salt Deposits, ref. [26].

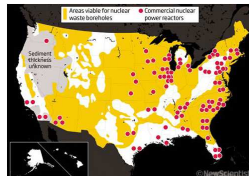


Figure 4 : U.S. Crystalline Basement, ref. [26].

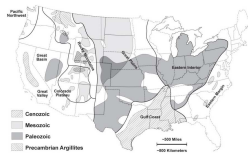


Figure 3 : U.S. Clay Deposits, ref. [11].



Figure 5 : U.S. Granite Beds, ref. [6].



Repository Components

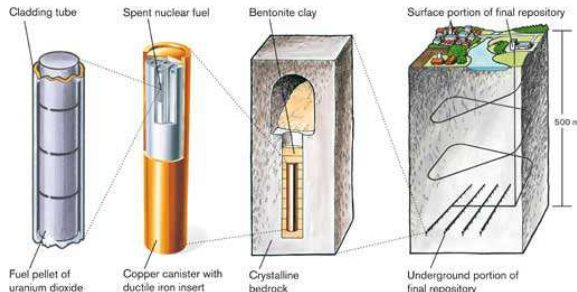


Figure 6 : Geologic disposal systems typically employ engineered barrier systems as well as natural barrier systems. This is a Swedish concept in granite [1].



Need For an Integrated Repository Model

Repository Capabilities within Systems Analysis Tools

Tool	Institution	Fuel Disposition	Radionuclide Transport	Heat Transport
NUWASTE[2]	NWTRB	yes	no	no
VISION [38]	INL	yes	no	YMR only
DANESS [34]	ANL	no	no	no
COSI [3]	CEA	yes	no	yes
NFCSim [31]	LANL	no	no	no
CAFCA [14]	MIT	no	no	no
ORION [14]	BNL	no	no	no
TSM [33]	OCRWM	yes	no	YMR only

Table 2 : System tools are lacking in radionuclide transport and heat transport calculations in generic geologic media.



Contributions from This Work

This work has provided a platform capable of bridging the gap between fuel cycle simulation and repository performance analysis.

- Conducted thermal transport sensitivity analyses. [19, 18]
- Conducted contaminant transport sensitivity analyses. [20]
- CYDER achieved integration with a fuel cycle simulator.
- Abstracted physical models of thermal and contaminant transport. [22]
- Demonstrated dominant physics of those models in CYDER, integrated with CYCLUS. [23, 17]
- Published source code, documentation, and testing to facilitate extension by external developers. [21]



Outline

① Motivation

- Future Fuel Cycle Options
- Geologic Disposal Concept Options
- Fuel Cycle Simulator Capabilities

② Modeling Paradigm

- Cyder Overview
- Thermal Transport in Cyder
- Radionuclide Transport in Cyder

③ Demonstration

- Radionuclide Transport Toy Cases
- Radionuclide Transport Validation Cases
- Thermal Transport Toy Cases
- Thermal Transport Validation Cases

④ Conclusion



Cyder Paradigm : Waste Stream Acceptance

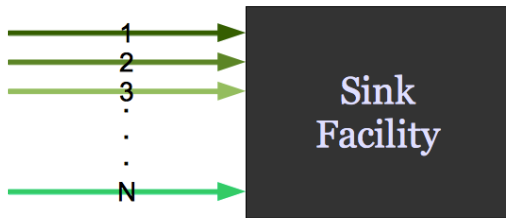


Figure 7 : To participate in a CYCLUS fuel cycle simulation, CYDER must accept arbitrary spent fuel and high level waste material data objects.



Cyder Paradigm : Waste Stream Conditioning

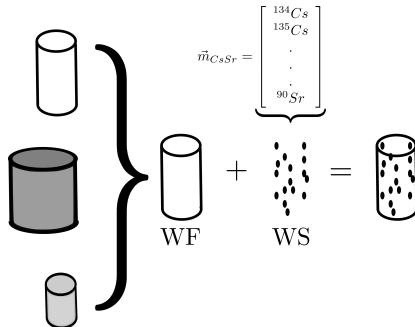


Figure 8 : In Cyder, discrete waste streams are conditioned into the appropriate discrete waste form according to user-specified pairings.



Cyder Paradigm : Waste Form Packaging

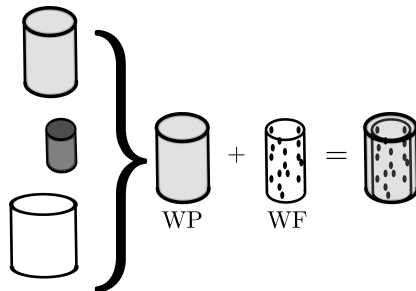


Figure 9 : In Cyder, one or more waste forms are loaded into the appropriate waste package according to user-specified pairings.



Cyder Paradigm : Waste Package Emplacement

Finally, the waste package is **emplaced** in a buffer component, which contains many other waste packages, spaced evenly in a grid. The grid is defined by the user input and depends on repository depth, Δz , waste package spacing, Δx , and tunnel spacing, Δy as in Figure 10.

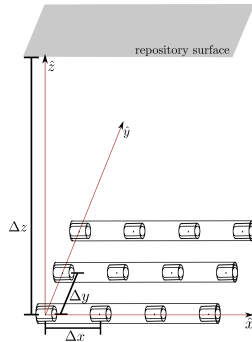


Figure 10 : The repository layout has a depth and a uniform package spacing.



Cyder Paradigm : Modularity

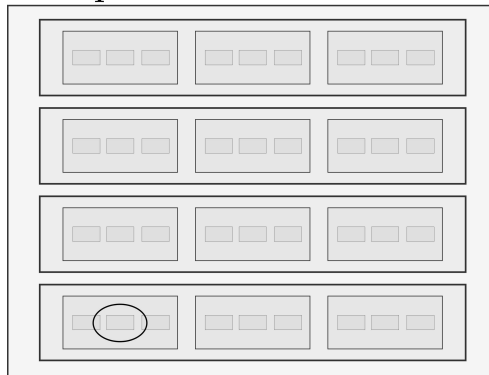
Components





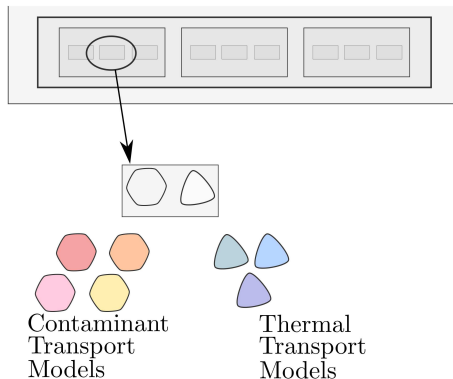
Cyder Paradigm : Modularity

Components





Cyder Paradigm : Modularity





Nested Components

Each Component has :

- a Geometry to describe its dimensions and location
- a NuclideModel for contaminant transport
- a ThermalModel for heat transport
- a Parent Component at its external barrier
- one or more Daughter Components at its internal barrier

Components have other data members such as a Type (WF, WP, BUFFER, FF), a material data table, a start date, etc.



Thermal Modeling in Cyder

Two types of thermal modeling occur in Cyder.

- The first is **capacity estimation** for waste stream acceptance.
- The next is **heat evolution** which determines heat evolution in the modules over repository lifetime.



Thermal Modeling in Cyder

Each can be achieved with one thermal model,

- This model employs a Specific Temperature Change algorithm [30, 29] and
- relies on a supporting **response database** combining detailed spent nuclear fuel composition data [8] with a detailed thermal repository performance analysis tool from Lawrence Livermore National Lab (LLNL) and the Used Fuel Disposition (UFD) campaign [12].
- This method is capable of rapid estimation of temperature increase near emplacement tunnels as a function of
 - waste composition,
 - limiting radius, r_{lim} ,
 - waste package spacing, S ,
 - near field thermal conductivity, K_{th} ,
 - and near field thermal diffusivity, α_{th} .



Specific Temperature Change Method

Introduced by Radel, Wilson et al., the Specific Temperature Change (STC) method uses a linear approximation to arrive at the thermal loading density limit [29, 30].

First, ΔT is determined for a limiting loading density of the particular material composition then it is normalized to a single kilogram of that material, Δt , the so called STC.

$$\Delta T(r_{lim}) = m \cdot \Delta t(r_{lim}) \quad (1)$$

where

ΔT = Temperature change due to m [K]

m = Mass of heat generating material [kg]

Δt = Temperature change due to 1 kg [K/kg]

r_{lim} = Limiting radius [m].



Specific Temperature Change Superposition

For an arbitrary waste stream composition, scaled curves, Δt_i , calculated in this manner for individual isotopes can be superimposed for each isotope to arrive at an approximate total temperature change.

$$\Delta T(r_{lim}) \sim \sum_i m_i \Delta t_i(r_{lim}) \quad (2)$$

where

i = An isotope in the material [-]

m_i = mass of isotope i [kg]

Δt_i = Specific temperature change due to i [K].



LLNL UFD MathCAD Model

The analytic model used to populate the reference dataset was created at LLNL for the UFD campaign [15, 13, 12]. It employs an analytic model from Carslaw and Jaeger and is **implemented in MathCAD** [7, 28]. The integral solver in the MathCAD toolset is the primary calculation engine for the analytic MathCAD thermal model, which relies on superposition of point, finite-line, and line source integral solutions.



Specific Temperature Change Calculations

A reference data set of temperature change curves was calculated. Repeated runs of a detailed model over the range of values in Table 3 determined Specific Temperature Change (STC) values over that range.

Thermal Cases

Parameter	Symbol	Units	Value Range
Diffusivity	α_{th}	[$m^2 \cdot s^{-1}$]	$1.0 \times 10^{-7} - 3.0 \times 10^{-6}$
Conductivity	K_{th}	[$W \cdot m^{-1} \cdot K^{-1}$]	0.1 – 4.5
Spacing	S	[m]	2, 5, 10, 15, 20, 25, 50
Radius	r_{lim}	[m]	0.1, 0.25, 0.5, 1, 2, 5
Isotope	i	[–]	$^{241,243}Am$, $^{242,243,244,245,246}Cm$, $^{238,240,241,242}Pu$, $^{134,135,137}Cs$, ^{90}Sr

Table 3 : A thermal reference dataset of STC values as a function of each of these parameters was generated by repeated parameterized runs of the LLNL MathCAD model[12, 13].



Scaling Demonstration

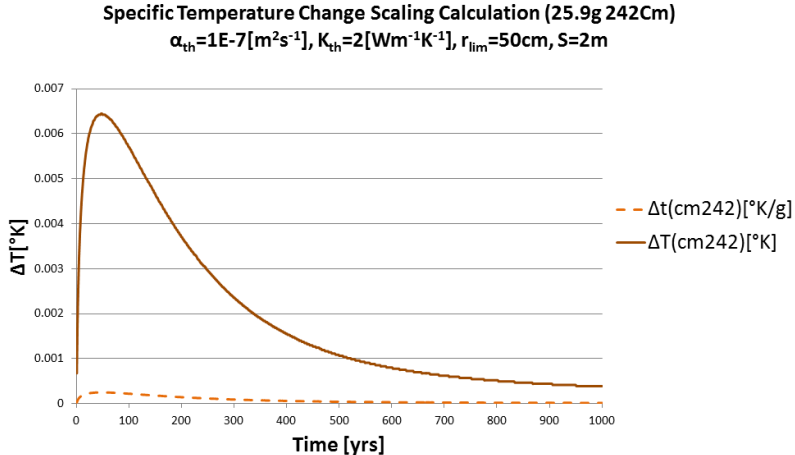


Figure 11 : As a demonstration of the calculation procedure, the temperature change curve for one initial gram of ^{242}Cm and is scaled to represent 25.9g, approximately the ^{242}Cm inventory per MTHM in 51GWD burnup UOX PWR fuel.



Superposition Concept

The supporting database was limited to some primary heat contributing isotopes present in traditional spent nuclear fuel, H , such that the superposition in equation (2) becomes

$$\Delta T(r_{lim}, S, K_{th}, \alpha_{th}) \sim \sum_{i \in H} m_i \Delta t_i(r_{lim}, S, K_{th}, \alpha_{th}) \quad (3)$$

where

$$\begin{aligned} H &= \text{set of high heat isotopes } [-] \\ S &= \text{uniform waste package spacing } [m] \\ K_{th} &= \text{thermal conductivity } [W \cdot m^{-1} \cdot K^{-1}] \\ \alpha_{th} &= \text{thermal diffusivity } [m^2 \cdot s^{-1}] \end{aligned} \quad (4)$$



Superposition Demonstration

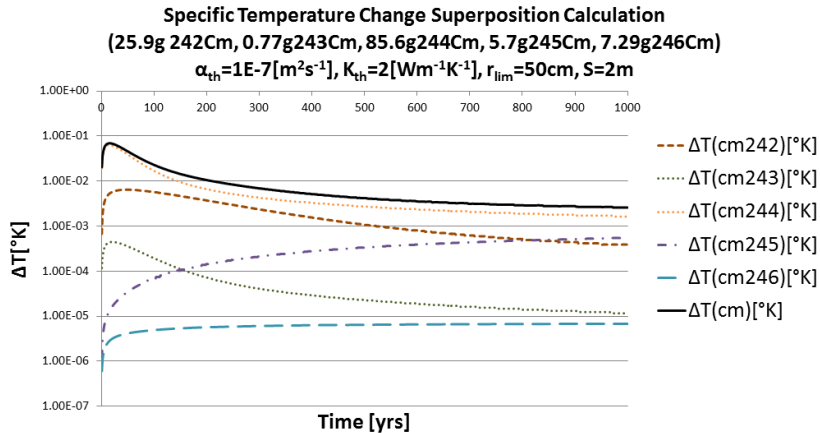


Figure 12 : As a demonstration of the calculation procedure, scaled temperature change curves for five curium isotopes are superimposed to achieve a total temperature change (note log scale).



Nested Components

The NuclideModel in a Component can be interchangeably represented by any of the four nuclide transport models.

- Degradation Rate Based Failure Model
- Mixed Cell with Degradation, Sorption, Solubility Limitation
- Lumped Parameter Model
- 1 Dimensional Approximate Advection Dispersion Solution, Brenner [4]



Clay GDSM Model

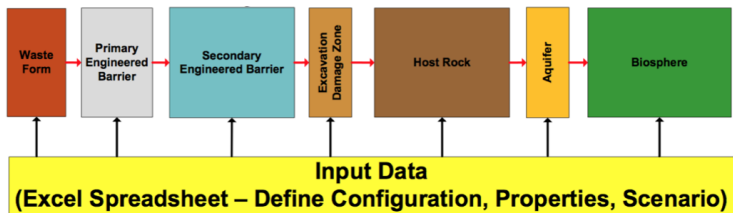


Figure 13 : The Clay Generic Disposal System Model (GDSM) was used for preliminary sensitivity analysis, abstraction iteration, and validation. This figure was reproduced from Figure 3.3-2 in [9].



Advection Dispersion Equation

In a saturated, reducing environment, contaminants are transported by **dispersion** and **advection** [32, 37, 35]:

$$\begin{aligned} J &= J_{dis} + J_{adv} \\ &= -\theta(D_{mdis} + \tau D_m)\nabla C + \theta vC \\ &= -\theta D\nabla C + \theta vC \end{aligned} \tag{5}$$

where

J_{dis} = Total Dispersive Mass Flux [$\text{kg}/\text{m}^2/\text{s}$]

J_{adv} = Advective Mass Flux [$\text{kg}/\text{m}^2/\text{s}$]

τ = Toruosity [-]

θ = Porosity [-]

D_m = Molecular diffusion coefficient [m^2/s]

D_{mdis} = Coefficient of mechanical dispersivity [m^2/s]

D = Effective Dispersion Coefficient [m^2/s]

C = Concentration [kg/m^3]

v = Fluid Velocity in the medium [m/s].



Timestepping Algorithm

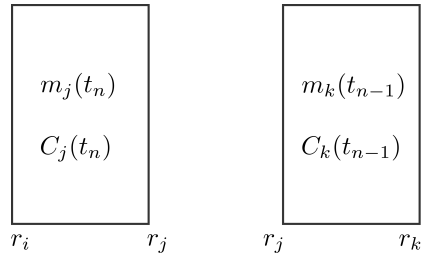


Figure 14 : Two components share an interface at r_j and contain mass and concentration profiles at the beginning of timestep t_n .



Timestepping Algorithm

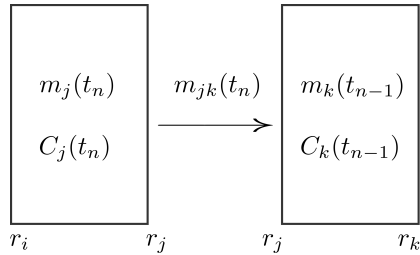


Figure 15 : The mass balance model in component k calculates the appropriate mass transfer based on boundary information from component j.



Timestepping Algorithm

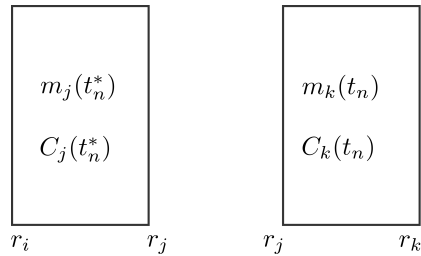


Figure 16 : Based on the mass transfer, both components update their mass and concentration profiles based on their mass balance model.



Radionuclide Transport: Degradation Rate Based Release

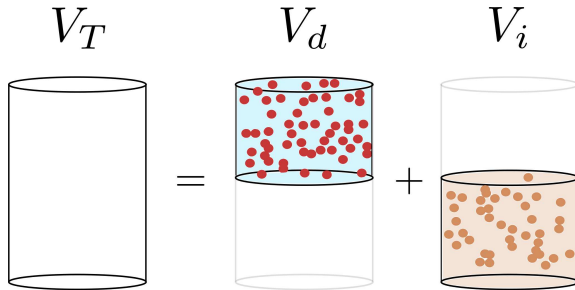


Figure 17 : The control volume contains an intact volume V_i and a degraded volume, V_d . Contaminants in V_d are available for transport, while contaminants in V_i are contained.



Radionuclide Transport : Mixed Cell with Sorption and Solubility

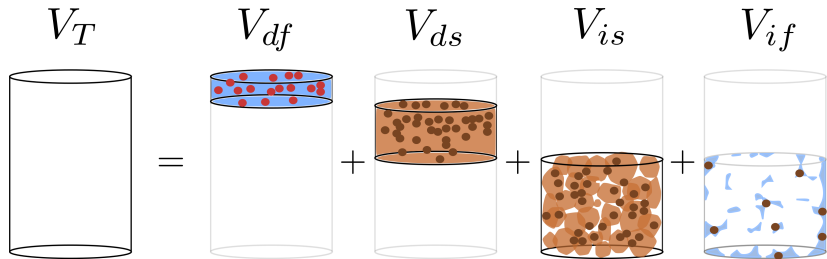


Figure 18 : The degraded volume is modeled as a solid degraded volume, V_{ds} , and a fluid degraded volume, V_{df} . The intact volume is modeled as an intact solid volume, V_{is} , and an intact fluid volume V_{if} . Only contaminants in V_{df} are available for transport.



Radionuclide Transport : Mixed Cell Sorption

The mass of contaminant sorbed into the degraded and precipitated solids can be found using a linear isotherm model [32], characterized by the relationship

$$s_i = K_{di} C_i \quad (6)$$

where

s_i = the solid concentration of isotope i [kg/kg]

K_{di} = the distribution coefficient of isotope i [m^3/kg]

C_i = the liquid concentration of isotope i [kg/m^3].



Radionuclide Transport : Mixed Cell Solubility Limitation

In addition to engineered barriers, contaminant transport is constrained by the solubility limit [16],

$$m_{s,i} \leq V_w C_{sol,i}, \quad (7)$$

where

$m_{s,i}$ = solubility limited mass of isotope i in volume V_w [kg]

V_w = volume of the solution [m^3]

$C_{sol,i}$ = solubility limit, the maximum concentration of i [kg/m^3].



Radionuclide Transport: Lumped Parameter Transport Model

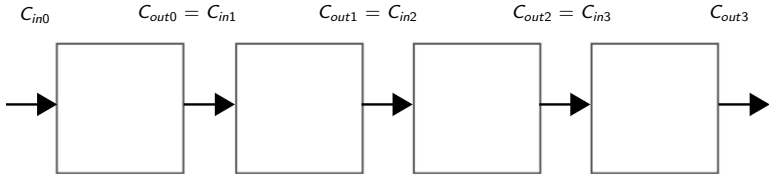


Figure 19 : The method by which each lumped parameter component is modeled is according to a relationship between the incoming concentration, $C_{in}(t)$, and the outgoing concentration, $C_{out}(t)$.

$$C_{out}(t) = \int_0^{\infty} C_{in}(t - t') g(t') e^{-\lambda t'} dt' \quad (8)$$

where

t' = time of entry [s]

$t - t'$ = transit time [s]

$g(t - t')$ = response function, a.k.a. transit time distribution [-]

λ = radioactive decay constant [s^{-1}].



Radionuclide Transport: Lumped Parameter Transport Model

Some response functions used commonly in chemical engineering applications include the Piston Flow Model (PFM), Exponential Model (EM), and the dispersion model (DM). The solutions to these for constant concentration at the source boundary are given in [25],

$$C(t) = \begin{cases} PFM & C_0 e^{-\lambda t_t} \\ EM & \frac{C_0}{1+\lambda t_t} \\ DM & C_0 e^{\frac{Pe}{2}} \left(1 - \sqrt{1 + \frac{4\lambda t_t}{Pe}} \right) \end{cases} \quad (9)$$



Radionuclide Transport: 1D Finite, Cauchy B.C.

$$-D \frac{\partial C}{\partial z} \Big|_{z=0} + vC = \begin{cases} vC_0 & t < t_0 \\ 0 & t > t_0 \end{cases} \quad \frac{\partial C}{\partial z} \Big|_L = 0$$

The diagram shows a horizontal line segment representing a 1D domain. The left endpoint is labeled $z = 0$. Above the segment, at the $z = 0$ position, is the equation $C(z, 0) = C_i$. The right endpoint is labeled $z = L$. Above the segment, at the $z = L$ position, is the equation $\frac{\partial C}{\partial z} \Big|_L = 0$.

Figure 20 : A one dimensional, finite, unidirectional flow, solution with Cauchy and Neumann boundary conditions [35, 4].



Radionuclide Transport: 1D Finite, Cauchy B.C.

For the boundary conditions,

$$-D \frac{\partial C}{\partial z} \Big|_{z=0} + v_z c = \begin{cases} v_z C_0 & (0 < t < t_0) \\ 0 & (t > t_0) \end{cases} \quad (10)$$

and

$$\frac{\partial C}{\partial z} \Big|_{z=L} = 0 \quad (11)$$

and the initial condition,

$$C(z, 0) = C_i, \quad (12)$$

the solution is given as

$$C(z, t) = \begin{cases} C_i + (C_0 - C_i) A(z, t) & 0 < t \leq t_0 \\ C_i + (C_0 - C_i) A(z, t) - C_0 A(z, t - t_0) & t \geq t_0. \end{cases} \quad (13)$$



Radionuclide Transport: 1D Finite, Cauchy B.C.

For the vertical flow coordinate system, A is defined as

$$\begin{aligned} A(z, t) = & \left(\frac{1}{2} \right) \operatorname{erfc} \left[\frac{Rz - vt}{2\sqrt{DRt}} \right] \\ & + \left(\frac{v^2 t}{\pi RD} \right)^{1/2} \exp \left[-\frac{(Rz - vt)^2}{4DRt} \right] \\ & - \frac{1}{2} \left(1 + \frac{vz}{D} + \frac{v^2 t}{DR} \right) \exp \left[\frac{vz}{D} \right] \operatorname{erfc} \left[\frac{Rz + vt}{2\sqrt{DRt}} \right] \\ & + \left(\frac{4v^2 t}{\pi RD} \right)^{1/2} \left[1 + \frac{v}{4D} \left(2L - z + \frac{vt}{R} \right) \right] \exp \left[\frac{vL}{D} - \frac{R}{4Dt} \left(2L - z + \frac{vt}{R} \right)^2 \right] \\ & - \frac{v}{D} \left[2L - z + \frac{3vt}{2R} + \frac{v}{4D} \left(2L - z + \frac{vt}{R} \right)^2 \right] \exp \left[\frac{vL}{D} \right] \operatorname{erfc} \left[\frac{R(2L - z) + vt}{2\sqrt{DRt}} \right] \end{aligned}$$

where

L = Extent of the solution domain [m]

R = Retardation factor [-].

Outline



① Motivation

- Future Fuel Cycle Options
- Geologic Disposal Concept Options
- Fuel Cycle Simulator Capabilities

② Modeling Paradigm

- Cyder Overview
- Thermal Transport in Cyder
- Radionuclide Transport in Cyder

③ Demonstration

- Radionuclide Transport Toy Cases
- Radionuclide Transport Validation Cases
- Thermal Transport Toy Cases
- Thermal Transport Validation Cases

④ Conclusion



Demonstration

- Unit Testing Framework
- Base (Toy) Cases
- Dominant Physics Validation Cases



Degradation Rate Model Base Case IV

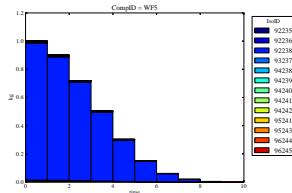


Figure 21 : WF 5 ($F_d = 0.1$) releases material with degradation.

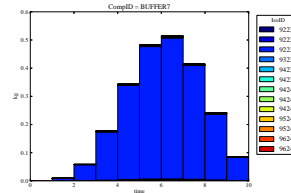


Figure 23 : Buffer 7 ($F_d = 0.1$), receives and then releases material.

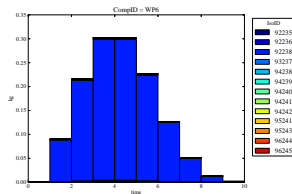


Figure 22 : WP 6 ($F_d = 0.1$) receives and releases material.

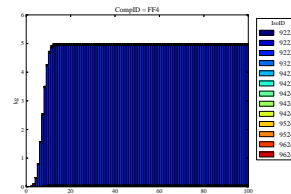


Figure 24 : Far Field 4 ($F_d = 0.0$), achieves total containment.



Degradation Rate Model Base Case IV

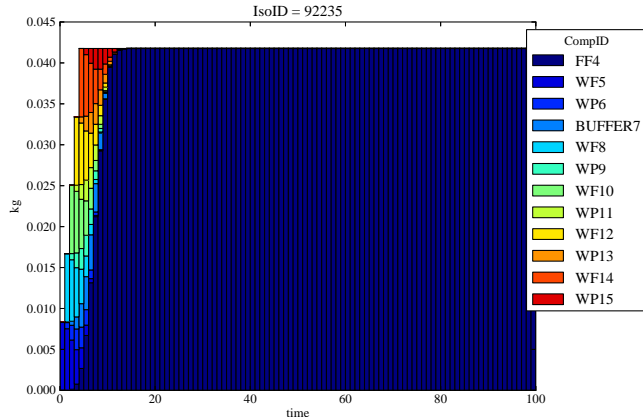


Figure 25 : For DRIV case in which total containment in the far field is assumed ($F_{d,\text{ff}} = 0$), ^{235}U travels through interior components ($F_d = 0.1$) before permanent residence in the far field component.



Mixed Cell Model Base Case II

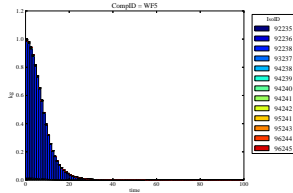


Figure 26 : WF 5 releases material with degradation.

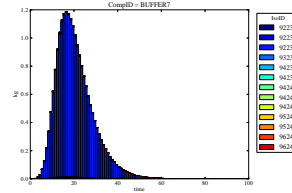


Figure 28 : Buffer 7, receives and releases material.

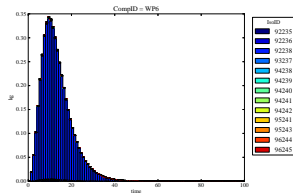


Figure 27 : WP 6 receives and releases material.

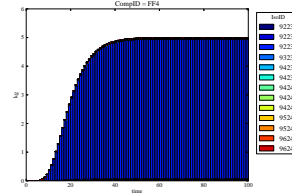


Figure 29 : Far Field 4 achieves total containment.



Mixed Cell Model Base Case II

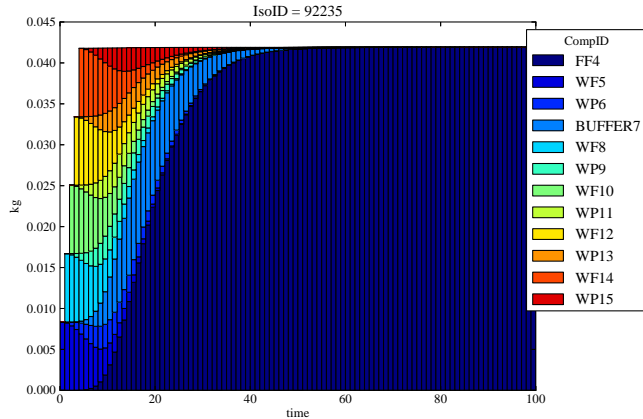


Figure 30 : For the MCII case in which containment is affected by solubility limitation, ($F_d = 0.1$, $S_{ref} = 0.1 \text{ kg/m}^3$ for all components), ^{235}U travels more slowly before permanent residence in the far field component.



Lumped Parameter Model Base Case

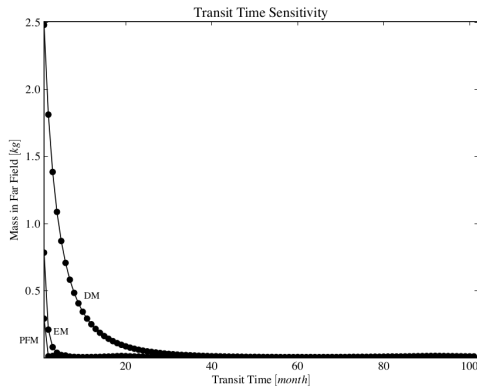


Figure 31 : The transit time parameterization of the lumped parameter model has a strong effect on the material reaching the far field after 30 months. The choice of model also strongly affects the results.



1D PPM Model Base Case I

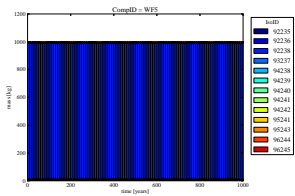


Figure 32 : WF 5 slowly releases material into WP 6.

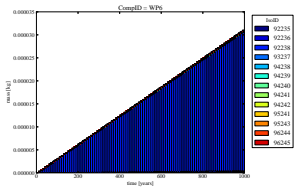


Figure 33 : Waste Package 6 slowly receives and releases material.

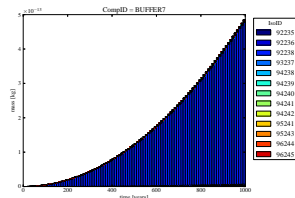


Figure 34 : Buffer 7 slowly receives and releases material.

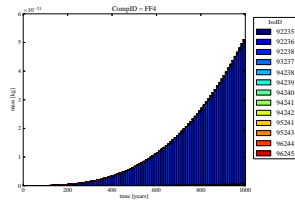


Figure 35 : Far Field 4 achieves total containment.



1D PPM Model Base Case I

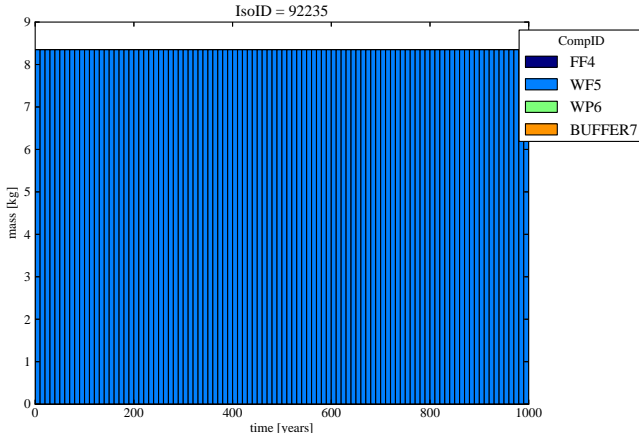


Figure 36 : For the case in which transport through all components is represented by the 1 Dimensional PPM model, material moves very slowly into the far field.



Clay GDSM Solubility Sensitivity

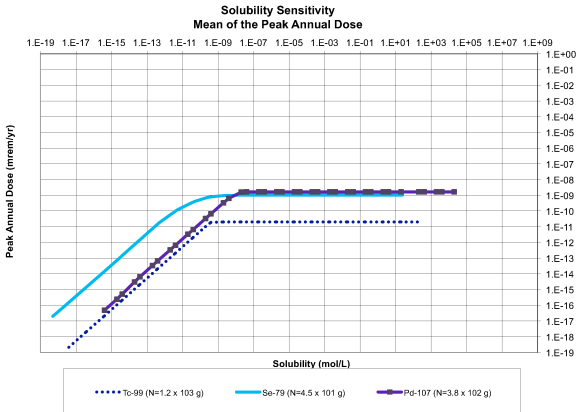


Figure 37 : Solubility limit sensitivity. The peak annual dose due to an inventory, N , of each isotope.



Cyder Solubility Sensitivity

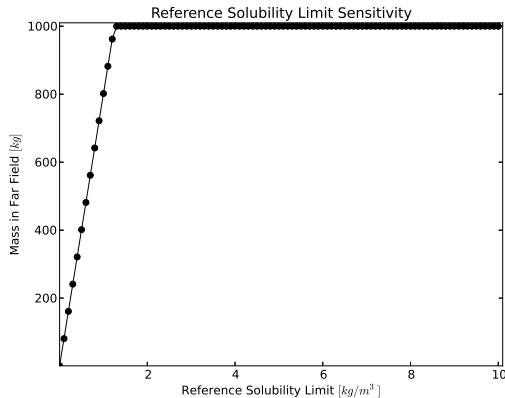


Figure 38 : Sensitivity demonstration of solubility limitation in CYDER for an arbitrary isotope assigned a variable solubility limit.



Clay GDSM Sorption Sensitivity

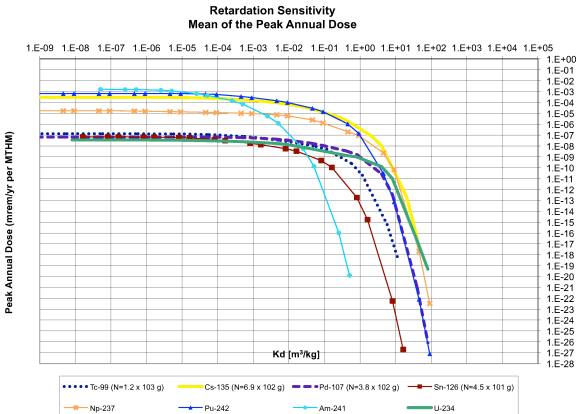


Figure 39 : K_d sensitivity. The peak annual dose due to an inventory, N , of each isotope.



Cyder Sorption Sensitivity

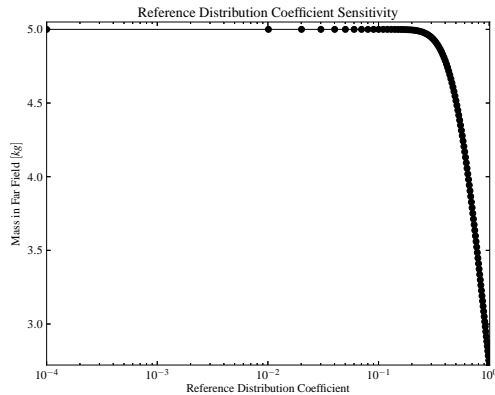
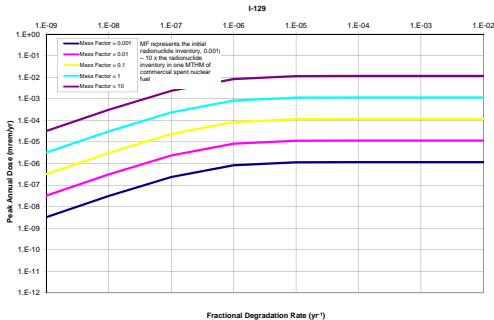


Figure 40 : K_d factor sensitivity in the CYDER tool for an arbitrary isotope assigned a variable K_d coefficient.



Clay GDSM Degradation Rate Sensitivity

Figure 41 : ^{129}I waste form degradation rate sensitivity.



Cyder Degradation Rate Sensitivity

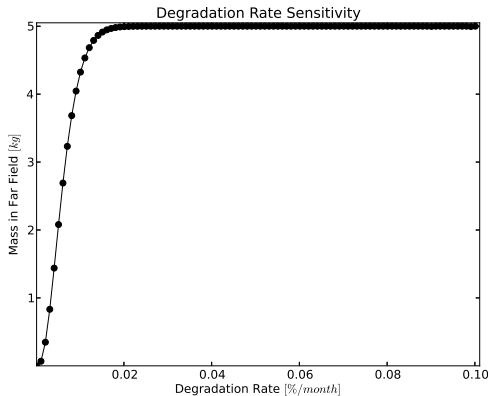


Figure 42 : Sensitivity demonstration of the degradation rate in CYDER for an arbitrary isotope.



Thermal Base Case Demonstration

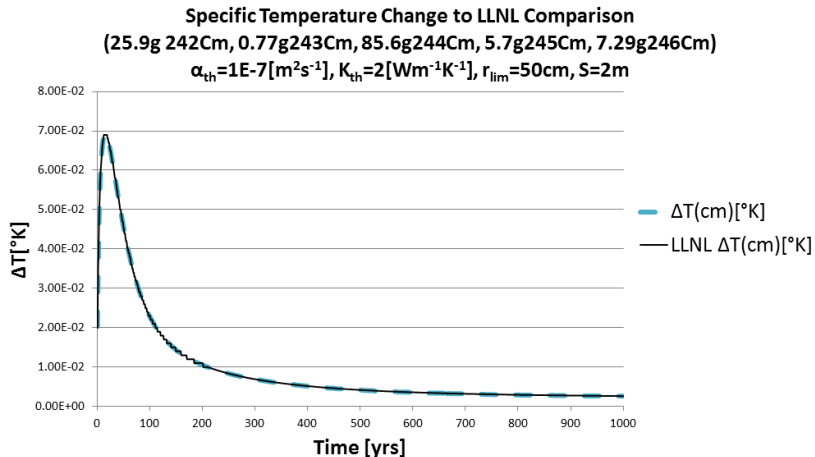


Figure 43 : This comparison of STC calculated thermal response from *Cm* inventory per MTHM in 51GWD burnup UOX PWR fuel compares favorably with results from the semi-analytic model from LLNL.



Thermal Base Case Demonstration

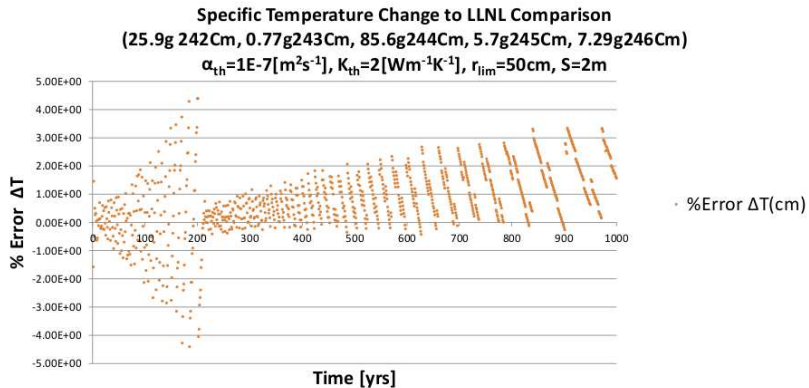


Figure 44 : Percent error between the semi-analytic model from LLNL and the STC calculated thermal response from *Cm* inventory per MTHM in 51GWD burnup UOX PWR fuel demonstrates a maximum percent error of 4.4%.



LLNL Model Thermal Conductivity Sensitivity

**Thermal Conductivity Sensitivity, LLNL Model Results,
 $t=30y$, $s=25m$, $r_{lim}=50cm$, 1kg Cm242 + Daughters**

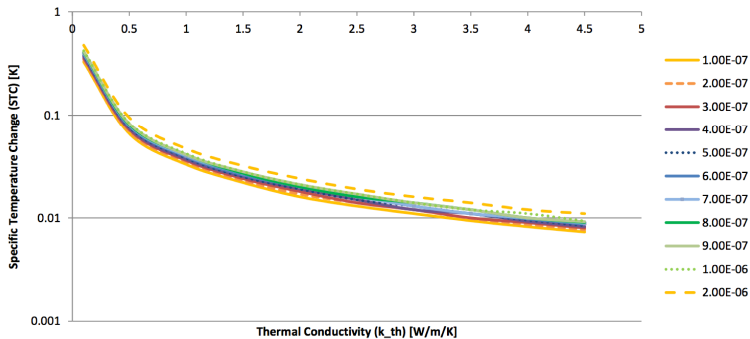


Figure 45 : Increased thermal conductivity decreases the temperature (here represented by STC) at the limiting radius.



Cyder Thermal Conductivity Sensitivity

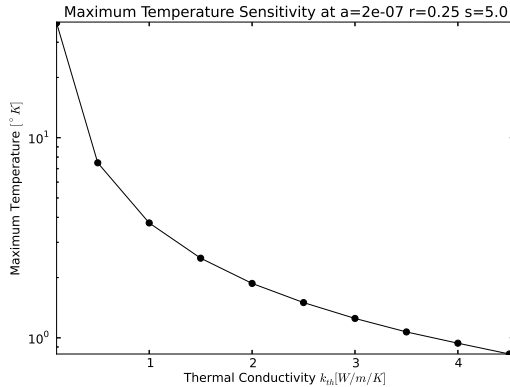


Figure 46 : Cyder results agree with those of the LLNL model. Increased K_{th} decreases temperature change at the limiting radius. The above example thermal profile results from 10kg of ^{242}Cm , $\alpha_{th} = 2 \times 10^{-7}$, $s = 5m$, and $r_{lim} = 0.25m$.



LLNL Model Thermal Diffusivity Sensitivity

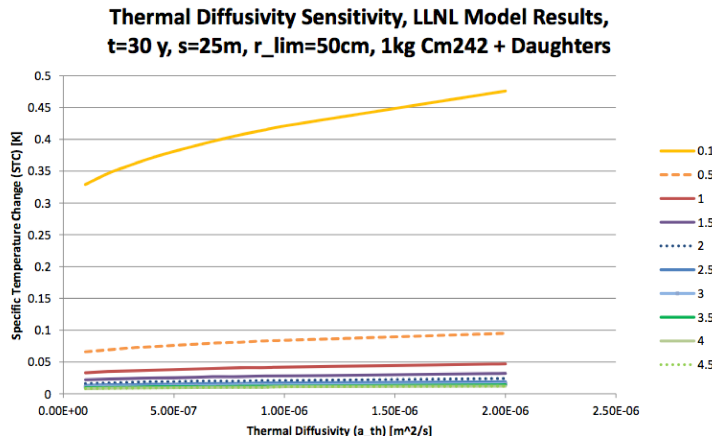


Figure 47 : Increased thermal diffusivity decreases temperature change (here represented by STC) at the limiting radius (here $r_{\text{calc}} = 0.5\text{m}$).



Cyder Thermal Diffusivity Sensitivity

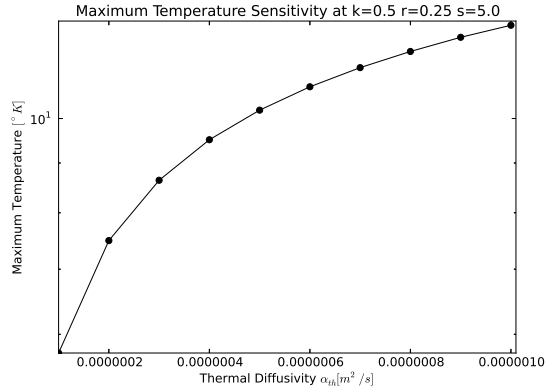


Figure 48 : Cyder trends agree with those of the LLNL model, in which increased thermal diffusivity results in reduced temperature change at the limiting radius. The above example thermal profile results from 10kg of ^{242}Cm .



Outline

① Motivation

- Future Fuel Cycle Options
- Geologic Disposal Concept Options
- Fuel Cycle Simulator Capabilities

② Modeling Paradigm

- Cyder Overview
- Thermal Transport in Cyder
- Radionuclide Transport in Cyder

③ Demonstration

- Radionuclide Transport Toy Cases
- Radionuclide Transport Validation Cases
- Thermal Transport Toy Cases
- Thermal Transport Validation Cases

④ Conclusion

Conclusion : Summary of Contributions



This work has provided a software platform capable of bridging the gap between fuel cycle simulation and repository performance analysis.

- Conducted thermal transport sensitivity analyses. [19, 18]
- Conducted contaminant transport sensitivity analyses. [20]
- CYDER achieved integration with a fuel cycle simulator.
- Abstracted physical models of thermal and contaminant transport. [22]
- Demonstrated dominant physics of those models in CYDER, integrated with CYCLUS. [23, 17]
- Published source code, documentation, and testing to facilitate extension by external developers. [21]



Conclusion : Suggested Future Work

Further work could include

- cultivation of a developer community,
- more detailed benchmarking validation against sophisticated tools,
- comparison against experimental data, where available,
- demonstration of dynamic fuel cycle feedback sensitivities,
- additional physics (fracture models, biosphere models),
- and additional supporting data.



Acknowledgements

I am grateful to a number of extraordinary professors and colleagues at the Universities of Wisconsin and Chicago, as well as the national laboratories, who have inspired and encouraged me. My advisor, **Prof. Paul P.H. Wilson**, my laboratory mentor, **Dr. W. Mark Nutt**, and my committee members, **Prof. Jean M. Bahr**, **Prof. Michael L. Corradini**, **Prof. Douglass L. Henderson**, and **Prof. Robert J. Witt**, were especially supportive in this endeavor.

So too, my colleagues **Kyle M. Oliver**, **Matthew J. Gidden** and **Robert W. Carlsen** as well as summer student **Alexander T. Bara** have been essential collaborators and contributors. All confidence I have in these results is owed to software practices inspired by my friends among The Hacker Within and Software Carpentry such as **Dr. Greg Wilson**, **Animal1**, **Wolfman**, **Slayer**, **Scopz**, **Nico**, **BlackBeard**, **BlondeBeard**, and **RedBeard**. I owe my sanity to **Dr. Denia Djokić**.

This work was carried out in the CNERG of the University of Wisconsin - Madison's EP Department and the UFD Campaign at ANL. This work is supported by the U.S. Department of Energy, Basic Energy Sciences, Office of Nuclear Energy, under contract # DE-AC02-06CH11357.



References I

- [1] Svensk kärnbranslehantering AB.
Long-term Safety for KBS-3 Repositories at Forsmark and Laxemar-a First Evaluation: Main Report of the SR-Can Project.
SKB, November 2006.
- [2] Mark Abkowitz.
Nuclear waste assessment system for technical evaluation - NUWASTE, October 2010.
- [3] Lionel Boucher.
International comparison for transition scenario codes involving COSI, DESAE, EVOLCODE, FAMILY and VISION, November 2010.
CEA France.
- [4] Howard Brenner.
The diffusion model of longitudinal mixing in beds of finite length. numerical values.
Chemical Engineering Science, 17(4):229–243, April 1962.
- [5] T.L. Bridges, A.L. Lengyel, D.K. Morton, and D.L. Pincock.
Standardized DOE spent nuclear fuel canister and transportation system for shipment to the national repository.
In *Proceedings of Waste Management 2001*, Tucson, February 2001.



References II

- [6] J. B. Bush.
Economic and technical feasibility study of compressed air storage.
Report ERDA, page 7676, 1976.
- [7] H. S. Carslaw and J. C. Jaeger.
Conduction of heat in solids.
Oxford: Clarendon Press, 1959, 2nd ed., 1, 1959.
- [8] J. T. Carter, A. J. Luptak, J. Gastelum, C. Stockman, and A. Miller.
Fuel cycle potential waste inventory for disposition.
Technical report, FCR&D-USED-2010-000031, Rev. 3, 2011.
- [9] Daniel Clayton, Geoff Freeze, Ernest Hardin, W. Mark Nutt, Jens Birkholzer, H.H. Liu, and Shaoping Chu.
Generic disposal system modeling - fiscal year 2011 progress report.
Technical Report FCRD-USED-2011-000184, U.S. Department of Energy, Sandia, NM, August 2011.
- [10] DOE.
WIPP hazardous waste facility permit community relations plan, 2013.



References III

- [11] Serge Gonzales and Kenneth Sutherland Johnson.
Shales and other argillaceous strata in the united states.
Technical report, Earth Resource Associates, Inc., Athens, GA (USA), 1985.
- [12] Harris Greenberg, James Blink, Massimiliano Fratoni, Mark Sutton, and Amber Ross.
Application of analytical heat transfer models of multi-layered natural and engineered barriers
in potential high-level nuclear waste repositories.
In *WM2012*, Phoenix, AZ, March 2012.
LLNL-CONF-511672.
- [13] Harris Greenberg, Montu Sharma, and Mark Sutton.
Investigations on repository near-field thermal modeling.
Technical report, Lawrence Livermore National Laboratory, 2012.
- [14] Laurent Guerin.
A Benchmark Study of Computer Codes for System Analysis of the Nuclear Fuel Cycle,
volume MIT-NFC-TR-105.
Massachusetts Institute of Technology. Center for Advanced Nuclear Energy Systems. Nuclear
Fuel Cycle Program, 2009.



References IV

- [15] Ernest Hardin, James Blink, Harris Greenberg, Mark Sutton, Massimo Fratoni, Joe Carter, Mark Dupont, and Rob Howard.
Generic repository design concepts and thermal analysis - 8.8.2011 draft.
Technical Report FCRD-USED-2011-000143, Department of Energy Office of Used Fuel Disposition, Sandia, August 2011.
- [16] A. Hedin.
Integrated analytic radionuclide transport model for a spent nuclear fuel repository in saturated fractured rock.
Nuclear Technology, 138(2), 2002.
- [17] Kathryn Huff.
Cyclus fuel cycle simulation capabilities with the cyder disposal system model (in press).
In *Proceedings of GLOBAL 2013*, Salt Lake City, UT, United States, October 2013.
- [18] Kathryn Huff and Theodore H. Bauer.
Benchmarking a new closed-form thermal analysis technique against a traditional lumped parameter, finite-difference method.
Technical Report FCRD-UFD-000142, Argonne National Laboratory, Argonne, IL, United States, July 2012.



References V

- [19] Kathryn Huff and Theodore H. Bauer.

Numerical calibration of an analytical generic nuclear repository heat transfer model.

In *Transactions of the American Nuclear Society*, volume 106 of *Modeling and Simulation in the Fuel Cycle*, pages 260—263, Chicago, IL, United States, June 2012. American Nuclear Society, La Grange Park, IL 60526, United States.

- [20] Kathryn Huff and Mark Nutt.

Key processes and parameters in a generic clay disposal system model.

In *Transactions of the American Nuclear Society*, volume 107 of *Environmental Sciences – General*, pages 208—211, San Diego, CA, November 2012. the American Nuclear Society.

- [21] Kathryn D. Huff.

Cyder : A generic geology repository performance library, 2013.

- [22] Kathryn D. Huff.

Hydrologic nuclide transport models in cyder, a geologic disposal software library.

In *WM2013*, Phoenix, AZ, February 2013. Waste Management Symposium.

- [23] Kathryn D. Huff and Alexander T. Bara.

Dynamic determination of thermal repository capacity for fuel cycle analysis.

In *Transactions of the American Nuclear Society*, volume 108, pages 123–126, Atlanta, GA, United States, June 2013.



References VI

- [24] P. Lisowski.
Global nuclear energy partnership.
In *Global Nuclear Energy Partnership Annual Meeting*, 2007.
- [25] Piotr Maloszewski and Andrzej Zuber.
Lumped parameter models for the interpretation of environmental tracer data.
Manual on mathematical models in isotope hydrology. IAEA-TECDOC-910, page 959, 1996.
- [26] NewScientist.
Where should the US store its nuclear waste?
NewScientist, April 2011.
- [27] Christophe Poinsot and Stphane Gin.
Long-term behavior science: The cornerstone approach for reliably assessing the long-term performance of nuclear waste.
Journal of Nuclear Materials, 420(13):182–192, January 2012.
- [28] ptc.
MathCAD engineering calculations software, 2010.



References VII

- [29] T. E Radel.
Repository modeling for fuel cycle scenario analysis.
University of Wisconsin – Madison, 2007.
- [30] Tracy E. Radel, Paul P.H. Wilson, R. M. Grady, and Theodore H. Bauer.
Effect of separation efficiency on repository loading values in fuel cycle scenario analysis codes.
American Nuclear Society, LaGrange Park, IL, 2007.
- [31] E. Schneider, M. Knebel, and W. Schwenk-Ferrero.
NFCSim scenario studies of german and european reactor fleets.
Technical report, LA-UR-04-4911, Los Alamos National Laboratory, 2004.
- [32] F. W. Schwartz and H. Zhang.
Fundamentals of ground water.
Environmental Geology, 45:10371038, 2004.
- [33] Stephen L. Turner.
Discrete modeling: OCRWM total system model DRAFT.
Fuel Cycle Technologies FCR&D-XXXX-2009-XXXXXX, Argonne National Laboratory,
Argonne, IL, United States, May 2010.



References VIII

- [34] L. Van Den Durpel, D. C. Wade, and Abdellatif Yacout.
DANESS: a system dynamics code for the holistic assessment of nuclear energy system strategies.
Proceedings of the 2006 System Dynamics Conference, 2006.
- [35] Martinus Th. Van Genuchten and W. J. Alves.
Analytical solutions of the one-dimensional convective-dispersive solute transport equation.
Technical Bulletin, 9(1661), 1982.
- [36] W. von Lensa, R. Nabbi, and M. Rossbach.
RED-IMPACT Impact of Partitioning, Transmutation and Waste Reduction Technologies on the Final Nuclear Waste Disposal.
Forschungszentrum Jülich, 2008.
- [37] Herbert Fan Wang and Mary P. Anderson.
Introduction to groundwater modeling.
Academic Press, 1982.
- [38] A. M. Yacout, J. J. Jacobson, G. E. Matthern, S. J. Piet, D. E. Shropshire, and C. Laws.
VISION – verifiable fuel cycle simulation of nuclear fuel cycle dynamics.
In *Waste Management Symposium*, 2006.



GDSM Model Advective Diffusive Sensitivity

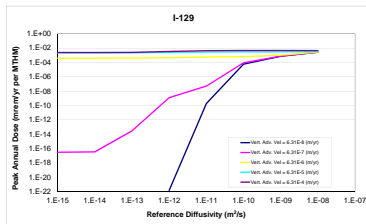


Figure 49 : ^{129}I / reference diffusivity sensitivity.

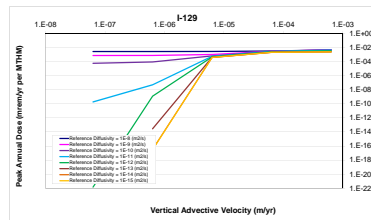


Figure 50 : ^{129}I / vertical advective velocity sensitivity.



Cyder Advective Diffusive Sensitivity

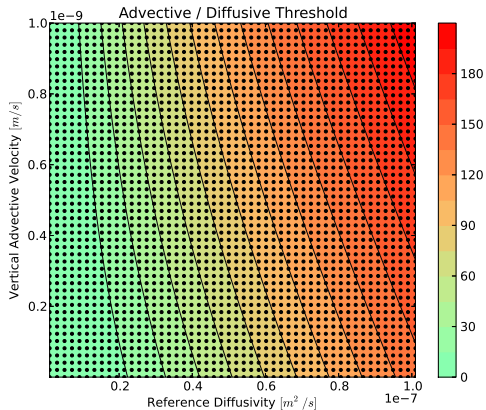


Figure 51 : Dual advective velocity and reference diffusivity sensitivity for a non-sorbing, infinitely soluble nuclide. This demonstration utilized the Degradation Rate model and the coupled advective dispersive mass transfer mode.

Outline



⑤ LLNL Model Background

Analytical Model Background

⑥ Geologic Media and Concepts

⑦ Mixed Cell Model



Analytical Model : Background

The analytical model

- was created at LLNL (H. Greenberg, J. Blink, et. al) [15, 13, 12]
- employs an analytic model from Carslaw and Jaeger [7]
- is implemented in MathCAD [28]
- seeks to inform heat limited waste capacity calculations for
 - arbitrary geology
 - arbitrary waste package loading densities
 - arbitrary homogeneous decay heat source



Analytical Model : Geometry

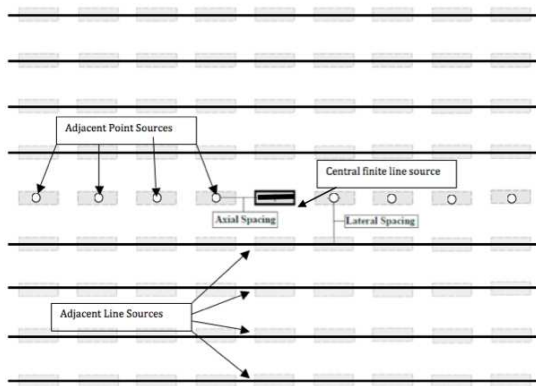


Figure 52 : Vertical, horizontal, alcove, and borehole emplacement layouts can be represented by a line of point sources and adjacent line sources [13].



Analytical Model : Calculation Method

LLNL's model is a MathCAD solution of the transient homogeneous conduction equation,

$$\nabla^2 T = \frac{1}{\alpha} \frac{\partial T}{\partial t}, \quad (14)$$

in which superimposed point and line source solutions approximate the repository layout.



Analytical Model : Calculation Method

The model consists of two conceptual regions, an external region representing the host rock and an internal region representing the waste form, package, and buffer Engineered Barrier System within the disposal tunnel wall.

- Since the thermal mass of the EBS is small in comparison to the thermal mass of the host rock, the internal region may be treated as quasi-steady state.
- The transient state of the temperature at the calculation radius is found with a convolution of the transient external solution with the steady state internal solution.
- The internal and external regions are **approximated** to be a single homogeneous medium.
- The process is then iterated with a one year resolution in order to arrive at a temperature evolution over the lifetime of the repository.



Analytical Model : Calculation Method

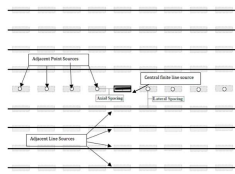


Figure 53 : The central package is represented by a finite line source [13].

The geometric layout of the analytic LLNL model in Figure 55 shows that the central package is represented by the finite line solution

$$T_{line}(t, x, y, z) =$$

$$\frac{1}{8\pi K_{th}} \int_0^t \frac{q_L(t')}{t - t'} e^{-\frac{(x^2+z^2)}{4\alpha(t-t')}} \cdot \left[\operatorname{erf} \left[\frac{1}{2} \frac{(y + \frac{L}{2})}{\sqrt{\alpha(t-t')}} \right] - \operatorname{erf} \left[\frac{1}{2} \frac{(y - \frac{L}{2})}{\sqrt{\alpha(t-t')}} \right] \right] dt'. \quad (15)$$



Analytical Model : Calculation Method

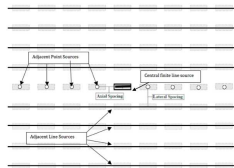


Figure 54 : Adjacent packages are represented as point sources [13].

Adjacent packages within the central tunnel are represented by the point source solution,

$$T_{point}(t, r) = \frac{1}{8K_{th}\sqrt{\alpha\pi^{\frac{3}{2}}}} \int_0^t \frac{q(t')}{(t - t')^{\frac{3}{2}}} e^{\frac{-r^2}{4\alpha(t-t')}} dt'. \quad (16)$$



Analytical Model : Calculation Method

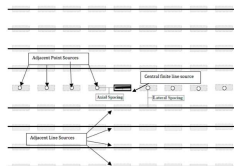


Figure 55 : The non-central disposal tunnels are represented as infinite line sources [13].

Adjacent disposal tunnels are represented by the infinite line source solution,

$$T_{\infty line}(t, x, z) = \frac{1}{4\pi K_{th}} \int_0^t \frac{q_L(t')}{t - t'} e^{-\frac{(x^2+z^2)}{4\alpha(t-t')}} \quad (17)$$

in infinite homogeneous media, where

$$\alpha = \text{thermal diffusivity } [m^2 \cdot s^{-1}]$$

$$q(t) = \text{point heat source } [W]$$

and

$$q_L(t) = \text{linear heat source } [W \cdot m^{-1}]$$

Superimposed point and line source solutions allow for a notion of the repository layout to be modeled in the host rock.



Outline

⑤ LLNL Model Background

Analytical Model Background

⑥ Geologic Media and Concepts

⑦ Mixed Cell Model



Clay Disposal Environments

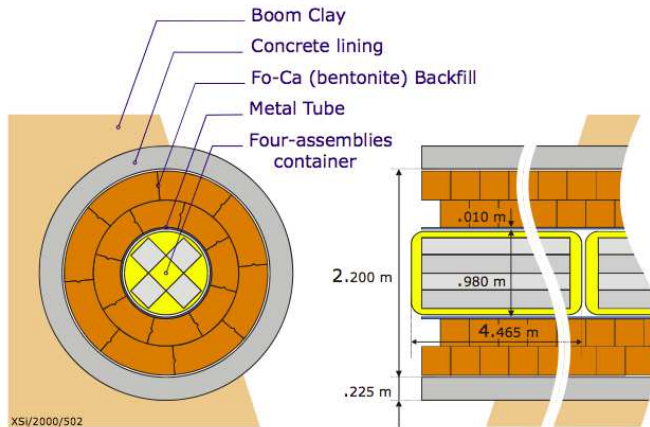


Figure 56 : Belgian reference concept in Boom Clay [36].



Granite Disposal Environments

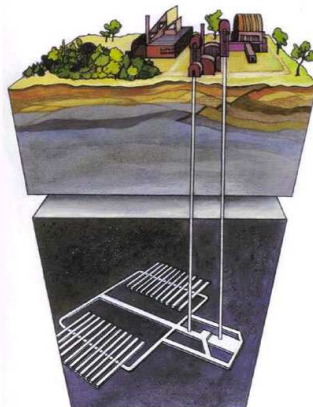


Figure 57 : Czech reference concept in Granite [36].



Salt Disposal Environments

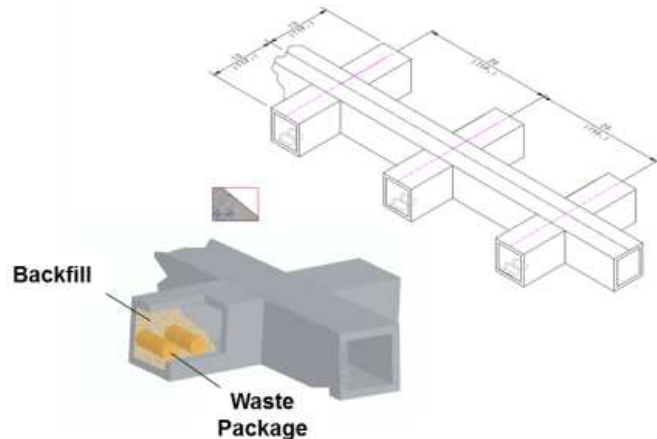


Figure 58 : DOE-NE Used Fuel Disposition Campaign concept in Salt [15].



Salt Disposal Environments

**Recess for
better heat
transfer**

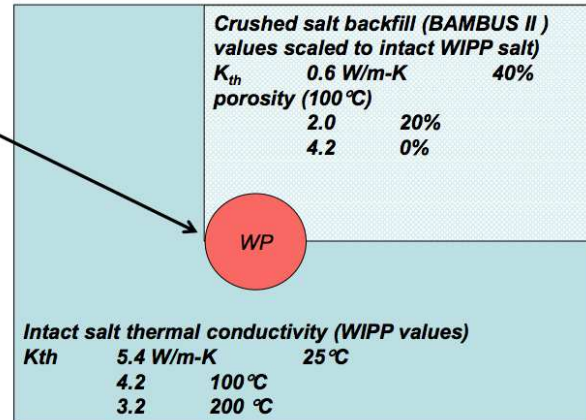


Figure 59 : DOE-NE Used Fuel Disposition Campaign concept in Salt [15].



Deep Borehole Disposal Environment

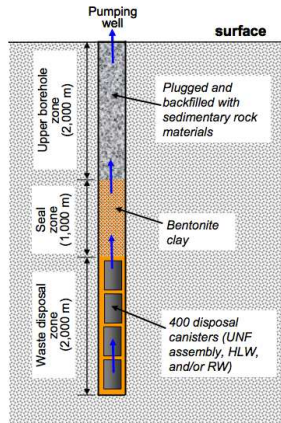


Figure 60 : DOE-NE Used Fuel Disposition Campaign Deep Borehole concept [15].



Engineered Barriers : Waste Forms

The first line of defense is the waste form.

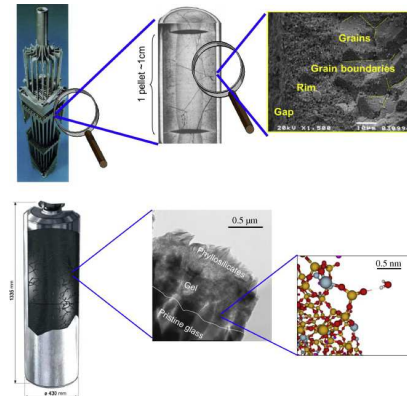


Figure 61 : A comparison of uranium oxide and borosilicate glass waste forms [27].



Engineered Barriers : Waste Packages

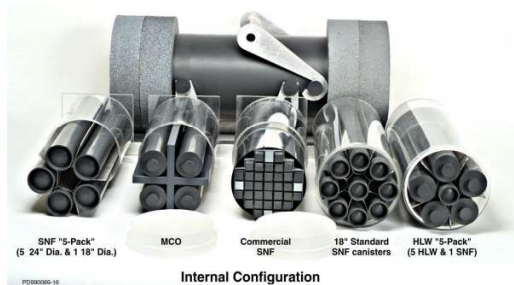


Figure 62 : Conceptual mockup of waste packages around waste forms [5].



Engineered Barriers : Disposal Cask

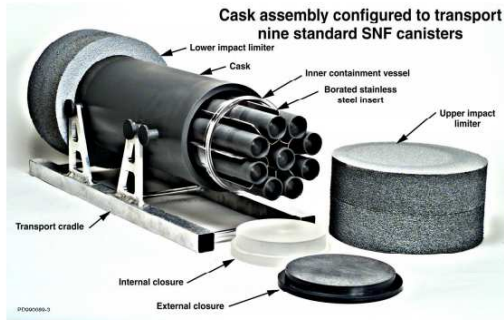


Figure 3. Conceptual design model.

Figure 63 : Conceptual mockup of a transport and disposal cask [5].



Engineered Barriers : Buffer

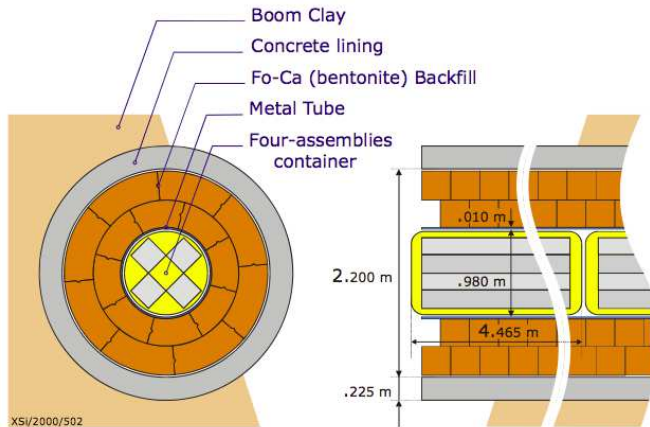


Figure 64 : Belgian reference concept in Boom Clay [36].



Natural Barrier : Geology

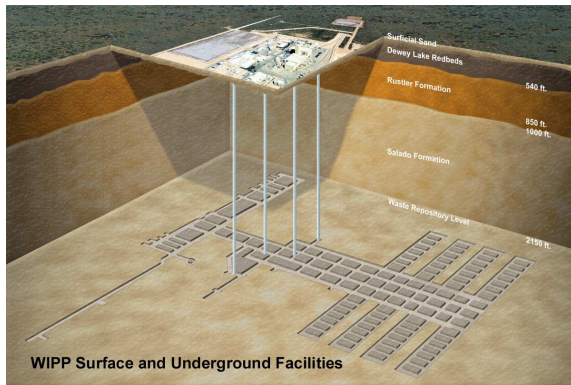
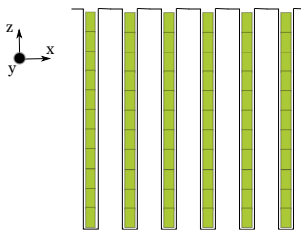


Figure 65 : The Waste Isolation Pilot Plant has many geologic layers above the salt bed [10].

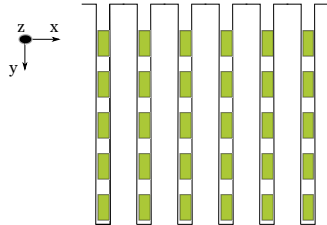


Repository Layouts

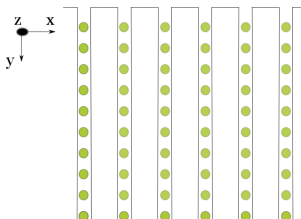
Deep Boreholes



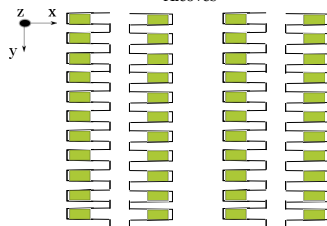
Horizontal In-Tunnel



Vertical In-Tunnel



Alcoves





Outline

⑤ LLNL Model Background

Analytical Model Background

⑥ Geologic Media and Concepts

⑦ Mixed Cell Model



Radionuclide Transport : Mixed Cell Sorption

The mass of contaminant sorbed into the degraded and precipitated solids can be found using a linear isotherm model [32], characterized by the relationship

$$s_i = K_{di} c_i \quad (18)$$

where

s_i = the solid concentration of isotope i [kg/kg]

K_{di} = the distribution coefficient of isotope i [m^3/kg]

c_i = the liquid concentration of isotope i [kg/m^3].

From the sorbed contaminant mass, we find the non-sorbed contaminant mass in the free fluid,

$$\begin{aligned} m_{ffl} &= m_{fft} - \frac{1}{2} \left(m_{fft} - m_{psm} - \frac{V_{ff}}{K_d} \right) \\ &\mp \frac{1}{2} \sqrt{m_{fft}^2 + 2m_{fft} \left(m_{psm} - \frac{V_{ff}}{K_d} \right) + \left(m_{psm} + \frac{V_{ff}}{K_d} \right)^2}. \end{aligned} \quad (19)$$

where

m_{fft} = total degraded contaminant mass [kg]

m_{psm} = noncontaminant mass in degraded and precipitated solids [kg]

m_{psc} = contaminant mass in degraded and precipitated solids [kg]

ρ_b = bulk (dry) density of the medium [kg/m^3].